4974 *Chem. Mater.* **2010,** *22,* 4974–4979
DOI:10.1021/cm101157w

CHEMISTRY OF MATERIALS
Article

Imine-Linked Microporous Polymer Organic Frameworks

Prativa Pandey, Alexandros P. Katsoulidis, Ibrahim Eryazici, Yuyang Wu, Mercouri G. Kanatzidis,* and SonBinh T. Nguyen*

Department of Chemistry, Northwestern University, 2145 Sheridan Road, Evanston, Illinois 60208-3113

Received April 25, 2010. Revised Manuscript Received June 30, 2010

Imine-linked microporous polymer organic frameworks (POFs) were synthesized via Schiff base condensation between 1,3,5-triformylbenzene and several readily available diamine monomers. Our facile, one-pot approach results in quantitative yields of POFs with the flexibility to incorporate several functional groups in their pores for tuning the interaction of their surface with different guest molecules. Synthesized POFs exhibit high specific surface areas (up to 1500 $m^2\ g^{-1}$) as well as high isosteric heats of H_2 adsorption (up to 8.2 kJ mol^{-1}).

Introduction

Metal-free microporous organic polymers[1−5] have recently attracted considerable attention because of their ease of synthesis, light weight, and high specific surface areas that allow for potential applications in gas storage[6−8] and gas separation.[9,10] These materials can be considered organic analogues of microporous materials like metal−organic frameworks (MOFs) and zeolites in terms of pore properties. They can be constructed using a plethora of organic reactions and building blocks,[10−14] which provides flexibility for the material design to achieve desirable pore properties (surface area, pore volume, pore width, etc.).[15−19] The highly cross-linked nature of these materials confer them with high thermal stability that is not commonly expected for organic polymers. Furthermore, the ability to incorporate various functional groups into microporous organic polymers can be advantageous for tuning the interaction of their surface with different types of guest molecules. Herein, we report a facile, one-pot, quantitative synthesis of imine-linked microporous polymer organic frameworks (POFs) having surface areas up to 1500 $m^2\ g^{-1}$. These materials also feature functional groups in their pores and have promising H_2 adsorption capability, with heat of H_2 adsorption up to 8.2 kJ mol^{-1}.

Experimental Section

Materials. Deuterated solvents were purchased from Cambridge Isotope Laboratories (Andover, MA). 3,5-Diaminophenol dihydrochloride (**B4**) (TCI America, Boston, MA) and 3,5-diaminobenzyl alcohol dihydrochloride (**B5**) (Aldrich Chemicals Co., Milwaukee, WI) were both free-based with sodium methoxide (see below) and isolated before use. All the gases used for the adsorption/desorption were ultra high purity grade 5 and were obtained from Airgas Specialty Gases (Chicago, IL). Synthesis of 1,3,5-triformylbenzene (**A1**) was synthesized with slight modification of a previously reported procedure (see Supporting Information).[20,21] All other chemicals and solvents were purchased from Aldrich Chemicals Co. (Milwaukee, WI) and used without further purification.

*To whom correspondence should be addressed. E-mail: m-kanatzidis@northwestern.edu (M.G.K.), stn@northwestern.edu (S.T.N.).

(1) Uribe-Romo, F. J.; Hunt, J. R.; Furukawa, H.; Klöck, C.; O'Keeffe, M.; Yaghi, O. M. *J. Am. Chem. Soc.* **2009**, *131*, 4570–4571.
(2) Schwab, M. G.; Fassbender, B.; Spiess, H. W.; Thomas, A.; Feng, X.; Müllen, K. *J. Am. Chem. Soc.* **2009**, *131*, 7216–7217.
(3) Tozawa, T.; Jones, J. T. A.; Swamy, S. I.; Jiang, S.; Adams, D. J.; Shakespeare, S.; Clowes, R.; Bradshaw, D.; Hasell, T.; Chong, S. Y.; Tang, C.; Thompson, S.; Parker, J.; Trewin, A.; Bacsa, J.; Slawin, A. M. Z.; Steiner, A.; Cooper, A. I. *Nat. Mater.* **2009**, *8*, 973–978.
(4) El-Kaderi, H. M.; Hunt, J. R.; Mendoza-Cortés, J. L.; Côté, A. P.; Taylor, R. E.; O'Keeffe, M.; Yaghi, O. M. *Science* **2007**, *316*, 268–272.
(5) Côté, A. P.; Benin, A. I.; Ockwig, N. W.; O'Keeffe, M.; Matzger, A. J.; Yaghi, O. M. *Science* **2005**, *310*, 1166–1170.
(6) Thomas, A.; Kuhn, P.; Weber, J.; Titirici, M. M.; Antonietti, M. *Macromol. Rapid Commun.* **2009**, *30*, 221–236.
(7) Ben, T.; Ren, H.; Ma, S.; Cao, D.; Lan, J.; Jing, X.; Wang, W.; Xu, J.; Deng, F.; Simmons, J. M.; Qiu, S.; Zhu, G. *Angew. Chem., Int. Ed.* **2009**, *48*, 9457–9460.
(8) Weber, J.; Antonietti, M.; Thomas, A. *Macromolecules* **2008**, *41*, 2880–2885.
(9) Farha, O. K.; Spokoyny, A. M.; Hauser, B. G.; Bae, Y.-S.; Brown, S. E.; Snurr, R. Q.; Mirkin, C. A.; Hupp, J. T. *Chem. Mater.* **2009**, *21*, 3033–3035.
(10) McKeown, N. B.; Budd, P. M. *Chem. Soc. Rev.* **2006**, *35*, 675–683.
(11) McKeown, N. B.; Budd, P. M.; Msayib, K. J.; Ghanem, B. S.; Kingston, H. J.; Tattershall, C. E.; Makhseed, S.; Reynolds, K. J.; Fritsch, D. *Chem.—Eur. J.* **2005**, *11*, 2610–2620.
(12) Budd, P. M.; Ghanem, B. S.; Makhseed, S.; McKeown, N. B.; Msayib, K. J.; Tattershall, C. E. *Chem. Commun.* **2004**, 230–231.
(13) Côté, A. P.; El-Kaderi, H. M.; Furukawa, H.; Hunt, J. R.; Yaghi, O. M. *J. Am. Chem. Soc.* **2007**, *129*, 12914–12915.
(14) Tsyurupa, M. P.; Davankov, V. A. *React. Funct. Polym.* **2006**, *66*, 768–779.
(15) Jiang, J. X.; Su, F.; Niu, H.; Wood, C. D.; Campbell, N. L.; Khimyak, Y. Z.; Cooper, A. I. *Chem. Commun.* **2008**, 486–488.
(16) Tilford, R. W.; Mugavero, S. J.; Pellechia, P. J.; Lavigne, J. J. *Adv. Mater.* **2008**, *20*, 2741–2746.
(17) Schmidt, J.; Werner, M.; Thomas, A. *Macromolecules* **2009**, *42*, 4426–4429.
(18) Weder, C. *Angew. Chem., Int. Ed.* **2008**, *47*, 448–450.
(19) Kuhn, P.; Krüger, K.; Thomas, A.; Antonietti, M. *Chem. Commun.* **2008**, 5815–5817.
(20) Dimick, S. M.; Powell, S. C.; McMahon, S. A.; Moothoo, D. N.; Naismith, J. H.; Toone, E. J. *J. Am. Chem. Soc.* **1999**, *121*, 10286–10296.
(21) Kaur, N.; Delcros, J. G.; Imran, J.; Khaled, A.; Chehtane, M.; Tschammer, N.; Martin, B.; Phanstiel, O. *J. Med. Chem.* **2008**, *51*, 1393–1401.

Published on Web 08/03/2010
© 2010 American Chemical Society

Procedure for Free-Basing 3,5-Diaminophenol Dihydrochloride and 3,5-Diaminobenzyl Alcohol Dihydrochloride. A 10-mL round-bottom flask equipped with a magnetic stir bar and either 3,5-diaminophenol dihydrochloride (2 mmol) or 3,5-diaminobenzyl alcohol dihydrochloride (2 mmol) was degassed using two evacuated-N_2-backfilled cycles. Under a nitrogen flow, dry methanol (5 mL) was added into the flask using a syringe. While stirring, sodium methoxide (4 mmol, 25 wt % in methanol) was added to the solution. After 10 min of stirring, the precipitated sodium chloride salt was slowly filtered through a conical funnel. The resulting filtrate was then concentrated to dryness on a rotary evaporator to obtain the desired free-based product **B4** (75% yield) or **B5** (62% yield).

Synthesis of POFs (A1-B1−A1-B6). *Condition I.* A 50-mL Schlenk flask equipped with a magnetic stir bar, a water-cooled reflux condenser, and a sand bath was degassed using two evacuation-N_2-backfill cycles. Under a nitrogen flow, 1,3,5-triformylbenzene and the appropriate solvent (enough to make solutions with concentrations of 0.34 to 0.8 M of aldehyde functional groups) were added into the flask. After 5 min of stirring, the amine monomer (1:1 ratio of aldehyde to amine functional group) was added as a solid under nitrogen. The temperature of the sand bath was increased to 180 °C over a period of 20 min. Bright-yellow to dark-brown solid precipitates were often observed within 10−30 min. The reaction was further refluxed under nitrogen atmosphere for 12, 24, or 48 h. Product isolation was carried out using the workup procedure listed below.

Condition II. A 50-mL Schlenk flask equipped with a magnetic stir bar, a water-cooled reflux condenser, and a sand bath was degassed using two evacuation-N_2-backfill cycles. Under a nitrogen flow, 1,3,5-triformylbenzene and the appropriate solvent (enough to make solutions with concentrations of 0.34 to 0.8 M of aldehyde functional groups) were added into the flask. After 5 min of stirring, the amine monomer (1:1 ratio of aldehyde to amine functional group) was added as a solid under nitrogen. The temperature of the sand bath was increased to 125 °C over the period of 20 min. Bright-yellow to dark-brown solid precipitates were often observed within 10−30 min. After 3 h, the reaction was either kept stirring at 125 °C under nitrogen for 21 h more or increased to 180 °C and further refluxed under nitrogen atmosphere for 24 h. Product isolation was carried out using the workup procedure listed below.

Condition III. A 50-mL Schlenk flask equipped with a magnetic stir bar, a water-cooled reflux condenser, and a sand bath was degassed using two evacuation-N_2-backfill cycles. Under a nitrogen flow, 1,3,5-triformylbenzene (202.7 mg) and dimethyl sulfoxide (DMSO) (5.3 mL, enough to make the final reaction solution having a concentration of 0.48 M aldehyde functional groups) were added into the flask. After 5 min of stirring, the amine monomer (202.7 mg, 1:1 ratio of aldehyde to amine functional group) dissolved in anhydrous DMSO (2.5 mL) was added at the rate of 0.1 mL per min at 50 °C using a syringe pump over 25 min, and then the temperature of the sand bath was slowly increased to 180 °C over a period of 20 min. As the temperature of the sand bath reaches 160 °C, sign of reflux can be seen inside the flask. Bright-yellow to dark-brown solid precipitates were often observed within 10−30 min. The reaction was further kept at 180 °C under nitrogen atmosphere for 24 h. Product isolation was carried out using the workup procedure listed below.

Workup Procedure. After the reaction was stopped and cooled down to room temperature, the reaction mixture was filtered over a Büchner funnel, and the precipitated solid was successively washed with anhydrous dimethyl formamide (DMF, 3 × 30 mL), anhydrous tetrahydrofuran (THF, 3 × 30 mL), and anhydrous methylene chloride (DCM, 3 × 50 mL). The resulting bright yellow to dark brown powder material was then dried under house vacuum at room temperature for 30 min. Yields averages between 90 and 95% for POF **A1-B2**.

End-Capping Experiment. End-capping experiments were performed to estimate the percentage of unreacted amine and aldehyde groups in POF **A1-B2** (Supporting Information, Table S1, entry 11). Aniline was used to cap the unreacted aldehyde groups, and benzaldehyde was used to cap the unreacted amine groups in the POF. Mesitylene was added to each reaction as an internal standard, and THF was used as a solvent for gas chromatographic (GC) analyses. Analysis of the reaction was carried out using FTIR spectroscopy, GC, and ^{13}C CPMAS NMR spectroscopy. N_2 adsorption−desorption measurements were also performed on the end-capped samples to confirm that the surface area is not affected by the end-capping experiments.

Preparation of Stock Solution of Capping Agents. Stock solution I (aniline-mesitylene): aniline (1167 μL, 12.8 mmol) and mesitylene (1781 μL, 12.8 mmol) were added to a flask containing THF (100 mL) and mixed well. Stock solution II (benzaldehyde-mesitylene): benzaldehyde (1304 μL, 12.8 mmol) and mesitylene (1781 μL, 12.8 mmol) were added to a flask containing THF (100 mL) and mixed well.

Control End-Capping Experiment. A 50-mL round-bottom flask was equipped with a magnetic stir bar, a water-cooled reflux condenser, and an oil bath. POF **A1-B2** (350 mg) and THF (25 mL) were added to the flask and stirred at 80 °C under N_2 for 24 h. During this period, aliquots from the supernatant were drawn for GC analyses. The final sample was then worked up as described above and subjected to ^{13}C CPMAS NMR and FTIR analyses.

End-Capping Experiment Using Aniline. A 50-mL round-bottom flask was equipped with a magnetic stir bar, a water-cooled reflux condenser, and an oil bath. POF **A1-B2** (350 mg) and stock solution I (25.8 mL) were added to the flask and stirred at 80 °C under N_2 for 24 h. During this period, aliquots from the supernatant were drawn for GC analyses. The final sample was then worked up as described above and subjected to ^{13}C CPMAS NMR and FTIR analyses.

End-Capping Experiment Using Benzaldehyde. A 50-mL round-bottom flask was equipped with a magnetic stir bar, a water-cooled reflux condenser, and an oil bath. POF **A1-B2** (350 mg) and stock solution II (25.8 mL) were added to the flask and stirred at 80 °C under N_2 for 24 h. During this period, aliquots from the supernatant were drawn for GC analyses. The final sample was then worked up as described above and subjected to ^{13}C CPMAS NMR and FTIR analyses.

Sample Preparation for GC Analysis. Aliquots (∼0.5 mL) of the supernatant were drawn from the end-capping reaction mixture (Supporting Information, Tables S6 and S7) and diluted with THF (10 mL). Aliquots of solutions were further diluted to 1/100th dilution prior to GC analysis. Consumption of the capping agent was determined by manual integration of the capping agent peak against mesitylene internal standard using pre-established response factors (via a calibration curve).

Sample Preparation for FTIR Analysis. The final solid products obtained after the end-capping experiments were dried and KBr pellets of those samples were prepared for FTIR analysis. The spectra were analyzed using EZ Omnic software. The peaks in the region 1500−1730 cm^{-1} were peak-fitted and integrated (Supporting Information, Tables S3−S5) using the SDP-XPS spectral data processing software (XPS International, Inc., Mountain View, CA).

Instrumentation. Fourier-transformed infrared (FTIR) spectroscopy was performed on a Thermo Nicolet Nexus 870 FTIR spectrometer (Thermo Scientific, Waltham, MA), using KBr pellets for all samples. Frequencies are given in reciprocal centimeters (cm^{-1}). TGA data were obtained with a Shimadzu TGA-50 thermal analyzer (Shimadzu Scientific Instruments, Coulmbia, MD) at a heating rate of 5 °C min^{-1} under nitrogen flow.

^{13}C cross-polarization, magic angle spinning (CPMAS) nuclear magnetic resonance spectra were recorded on a VNMRS 400 MHz spectrometer (Varian, Inc., Palo Alto, CA) (400 MHz for ^{1}H, 100.7 MHz for ^{13}C) equipped with a 5-mm HXY T3 PENCIL probe. The samples packed into a standard 5-mm (external diameter) zirconia rotor with a volume of 160 uL and capped by a Teflon spacer. All the spectra were obtained at the spinning rate of 10 kHz except for the spectrum displayed in Supporting Information, Figure S3b, which was obtained at 12 kHz spinning rate. Spectra were acquired using a $^{1}H-^{13}C$ CP contact time of 1.5 ms, acquisition time of 20 ms, and a recycle delay of 3 s between scans. High-power, two-pulse phase-modulation (TPPM) ^{1}H decoupling was applied during data acquisition to ensure the sharper peaks. The number of scans varied from 4 to 10000 depending on the compound being analyzed. ^{13}C NMR chemical shifts are reported in ppm downfield relative to tetramethylsilane (TMS) as zero ppm, calibrated using adamantane (38.3 ppm) as a secondary standard. All the spectra were acquired with neat powdered samples at room temperature. All the data were processed by VnmrJ software with a line broadening of 20 Hz.

Gas chromatographic (GC) analyses of reaction mixtures in capping studies were carried out on a Agilent 6890 Network instrument (Agilent Technologies, Santa Clara, CA) equipped with a flame-ionization detector (FID) interfaced to a Wintel PC using ChemStation Software (Version D.01.02, Agilent Technologies, Santa Clara, CA). The column used was a 30-m HP-5 capillary column with a 0.32-mm inner diameter and a 0.25-μm film thickness. Flow rate (He) = 0.9 mL min^{-1}.

All low-pressure (up to 1 bar) adsorption and desorption measurements were performed on a Micromeritics ASAP 2020 system (Micromeretics, Norcross, GA). Between 100 and 200 mg of samples were employed in each measurement, and the data were analyzed using the ASAP 2020 software (Micromeretics, Norcross, GA). Before measurement, samples were degassed for 10 h at 120 °C under high vacuum ($< 10^{-4}$ mbar). N_2 adsorption and desorption isotherms were measured at 77 K. The specific surface areas for N_2 were calculated using the Brunauer−Emmet−Teller (BET) model in the range of $0.01 < P/P_0 < 0.1$. The pore size distributions were calculated from the adsorption isotherms by nonlocal density functional theory (NLDFT). CO_2 adsorption isotherms were measured at 273 K. The specific surface areas for CO_2 were calculated using the Dubinin−Radushkevich model in the range of $0.0001 < P/P_0 < 0.03$. The micropore volumes obtained in both types of measurements were calculated using the Dubinin−Raduskevich model. High-pressure (up to 70 bar) H_2 uptake measurements were performed at 77 K using HPVA-100 (VTI Scientific Instruments, Hialeah, FL).

Low-pressure H_2 uptake measurements were performed at 77 and 87 K.[22] The collected data for each sample was fitted to the virial eq 1:

$$\ln p = \ln v + \frac{1}{T}\sum_{i=0}^{n1} a_i v^i + \sum_{i=0}^{n2} b_i v^i \qquad (1)$$

where p is the pressure in mm Hg, v is the adsorbed amount in mmol g^{-1}, T is the temperature in K, and a_i and b_i are adjustable parameters. The isosteric heat of H_2 adsorption, Q_{st}, was calculated according to eq 2:

$$q_{st} = -R\sum_{i=0}^{n1} a_i v^i \qquad (2)$$

where R is the gas constant (8.314 J mol^{-1} K^{-1}).

Scanning electron microscopy (SEM) images was obtained using a Leo 1525 scanning electron microscope (Carl Zeiss Micro-Imaging Inc., Thornwood, NY) with an accelerating voltage of 20 kV. Finely ground POF sample was prepared for analysis by dispersing onto a double sticky carbon tape (Ted Pella Inc., Redding, CA) attached to a flat aluminum sample holder. The samples were then coated with a gold−palladium film to facilitate conduction using a Denton Desk II (Denton Vacuum, Moorestown, NJ) sputter coater operating under argon atmosphere at 25 °C and ~25 mTorr.

Results and Discussion

We prepared POFs via Schiff base condensation using readily synthesized 1,3,5-triformylbenzene (**A1**) and various commercially available diamines (**B1-B6**) (Scheme 1). Combining these two classes of monomers in solution at high temperature led to powder products that are yellow, indicative of imine formation. Because the specific surface area of POF **A1-B2**, prepared using meta-diamine **B2**, was higher than POF **A1-B1**, prepared using para-diamine **B1** (Table 1, entries 2a and 1, respectively), we focused on meta-diamines (**B2-B6**) as the amine building blocks most likely to give rise to materials with high surface areas. In addition, we selected the reaction of trialdehyde **A1** with meta-diamine **B2** to examine the effect of monomer concentration, reaction temperature and time, solvent, and the rate of monomer addition, to maximize surface area and micropore volume (Table 1 and Supporting Information, Table S1).

Within the range of monomer concentrations attempted (0.34 to 0.80 M of amine functional groups, 1:1 ratio of aldehyde to amine functional groups), those below 0.40 and above 0.60 M yielded materials with lower surface areas, ~800 m^2 g^{-1} (Supporting Information,

Scheme 1. Synthesis of POFs via Schiff Base Condensation Polymerization

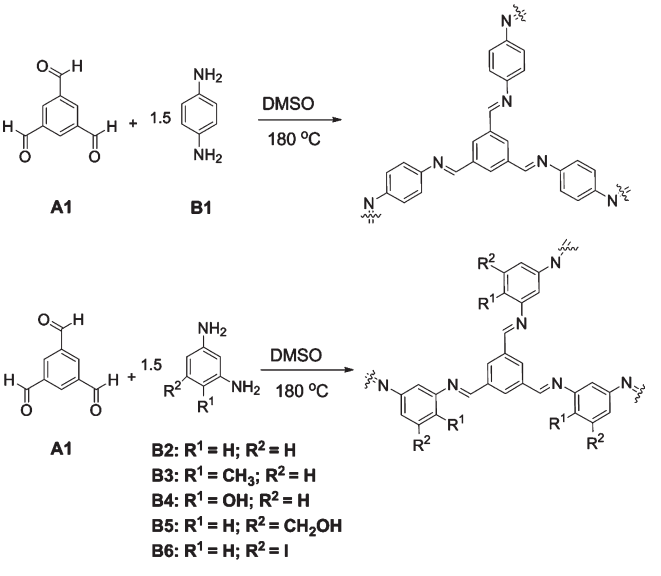

(22) Czepirski, L.; Jagiello, J. *Chem. Eng. Sci.* **1989**, *44*, 797–801.

Table 1. Surface Areas and Pore Properties of Imine-Linked POFs

entry	polymer[a]	specific surface area ($m^2\ g^{-1}$)	micropore volume ($cm^3\ g^{-1}$)	total pore volume ($cm^3\ g^{-1}$)	yield (%)
1	**A1-B1**[b,e]	466	0.14	0.32	89
2a	**A1-B2**[b,e]	1063	0.31	1.13	98
2b	**A1-B2**[c,e]	1051	0.31	1.01	96
2c	**A1-B2**[d,e]	583	0.19	0.43	71
2d	**A1-B2**[f]	***1521***	***0.45***	***1.13***	***98***
3	**A1-B3**[b,e]	723	0.25	0.60	87

[a] All reactions were carried out in DMSO and at 0.48 M aldehyde functional group concentration. [b] Reactions were carried out at 180 °C for 24 h (Condition I). [c] Reaction was carried out at 180 °C for 48 h (Condition I). [d] Reaction was carried out at 125 °C for 24 h (Condition II). [e] Both monomers were combined together within 5 min at the beginning of the reaction. [f] A solution of amine monomer was slowly added to a trialdehyde solution over 25 min at 50 °C at the beginning of the reaction, and the resulting mixture was heated at 180 °C for 24 h (Condition III).

Table S1, entries 12−16). Therefore, monomer concentration of 0.48 M was used for further optimization of reaction time, temperature, and solvent. When the synthesis was carried out at 125 °C for 24 h, the surface area for POF **A1-B2** was only 583 $m^2\ g^{-1}$ (Table 1, entry 2c) and the POF was isolated in low yield (71%). However, when the synthesis was carried out at temperatures between 160 and 190 °C (Supporting Information, Table S1, entries 6 and 9−11), the surface area of **A1-B2** increased significantly, to 1063 $m^2\ g^{-1}$ (Table 1, cf. entries 2a and 2c). At this high temperature range of 160−190 °C, the reaction reaches quantitative yields (~98%) within 24 h. If the reaction is stopped prematurely at 12 h, low-molecular-weight soluble materials still exist in solution as indicated by the yellow color of the supernatant liquid; in this case, the POF was isolated in lower yield (65%) and had lower surface area of 865 $m^2\ g^{-1}$ (Supporting Information, Table S1, entry 5).

Among the various solvents tested (DMF, DMSO, *N*-methyl-2-pyrrolidone (NMP), 1,4-dioxane, mesitylene), DMF and DMSO gave the best yields and surface areas (Supporting Information, Table S1, entries 4 and 6, respectively). In contrast, the less polar solvents mesitylene and dioxane gave either non-porous solids or solids with very low surface areas (Supporting Information, Table S1, entries 1 and 2). Presumably, these low-polarity solvents caused premature precipitation of the imine oligomers before they have a chance to cross-link and form significant pores (see further discussion below). On the basis of these results, we selected the most optimized reaction condition as 0.48 M amine monomer concentration in DMSO at 180 °C for 24 h under nitrogen atmosphere.

A lower surface area of 1063 $m^2\ g^{-1}$ (Table 1, entry 2a) was initially obtained by combining monomer **B2** with **A1** at the beginning of the reaction. Notably, slowly adding monomer **B2** to a solution of **A1** at 50 °C over a period of 25 min and then letting the reaction go to completion at 180 °C significantly increased this surface area by ~50%, to 1521 $m^2\ g^{-1}$, which is the highest specific surface area obtained for POFs **A1-B2** (Table 1, entry 2d). During the initial low-temperature addition phase, the reaction does not become as viscous as that in the case where both the monomers were added at the beginning. Presumably, the slower addition facilitates formation of more oligomers at the beginning of the reaction, which subsequently link up to form the microporous network structure in a less rapid manner and allow for the formation of POFs with higher surface areas (Table 1, cf. entries 2a and 2d). This is consistent with our observation that non-polar solvents afforded solid with low surface areas (see above).

The FTIR spectra of POFs **A1-B2** (Table 1, entries 2a and 2d) exhibited a strong imine (C═N) stretch at 1620 cm^{-1}, clearly confirming the formation of imine bonds. However, a carbonyl (C═O) stretch at 1690 cm^{-1} can also be observed, indicating the presence of unreacted aldehyde (Figure 1). Unreacted amine groups are also present, as indicated by the two broad spikes at 3300−3700 cm^{-1} region. The ^{13}C cross-polarization magic angle spinning (CPMAS) NMR spectrum of POF **A1-B2** (Table 1, entry 2a) further confirmed the presence of imine bonds with C═N resonance at 160 ppm that matches well with the C═N resonance of the diimine model compound **MC1** (Figure 2). A carbonyl peak was also observed at 195 ppm, attributed to unreacted aldehyde groups.

End-capping experiments with either aniline or benzaldehyde were carried out to gauge the amount of unreacted amine and aldehyde groups present in POF **A1-B2**

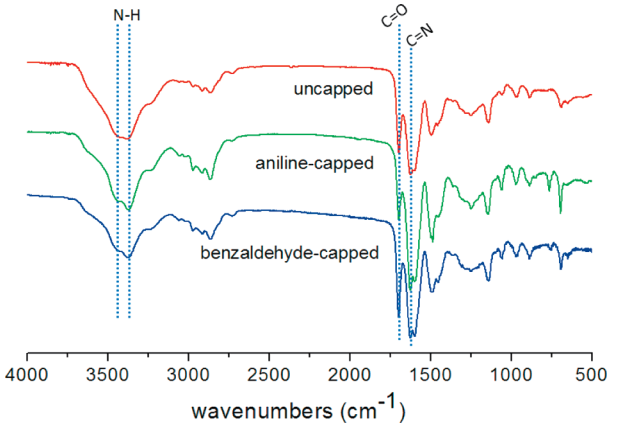

Figure 1. FTIR spectra of uncapped POF **A1-B2** (Supporting Information, Table S2, entry 1), aniline-capped POF **A1-B2** (Supporting Information, Table S2, entry 2), and benzaldehyde-capped POF **A1-B2** (Supporting Information, Table S2, entry 3).

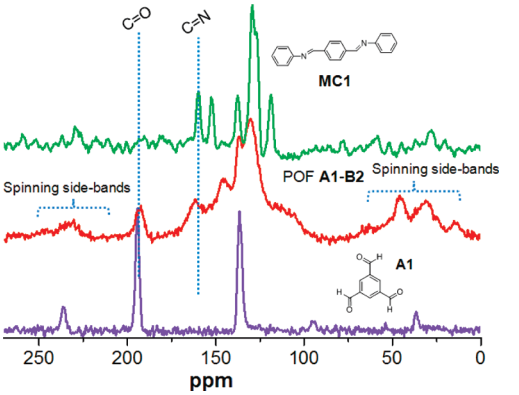

Figure 2. ^{13}C CPMAS NMR spectra of the diimine model compound (**MC1**), POF **A1-B2** (Table 1, entry 2a), and 1,3,5-triformylbenzene (**A1**).

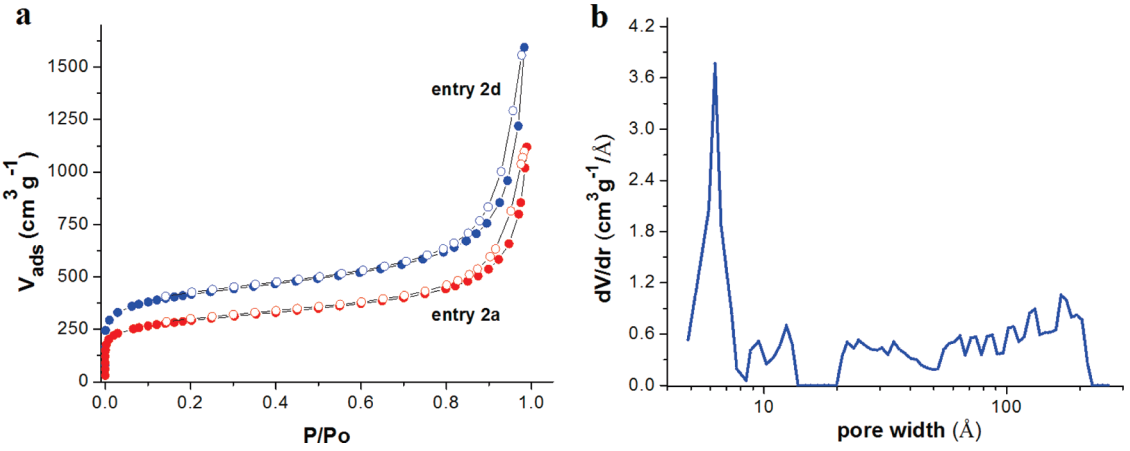

Figure 3. (a) N_2 adsorption−desorption isotherms of POFs **A1-B2** (Table 1, entries 2a and 2d) at 77 K. (b) Pore size distribution of POF **A1-B2** (Table 1, entry 2d) according to NLDFT analysis.

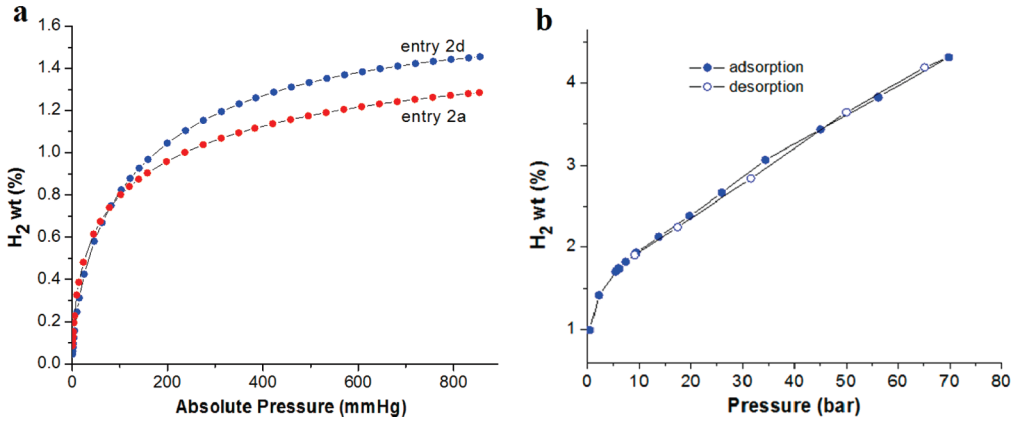

Figure 4. (a) H_2 adsorption isotherms of POFs **A1-B2** (Table 1, entries 2a and 2d) at 77 K. (b) H_2 adsorption isotherm of POF **A1-B2** (Table 1, entry 2d) at 77 K, up to 70 bar.

(Supporting Information, Table S1, entry 11). Most of the consumption of the capping agents occurred during the first 18 h (Supporting Information, Tables S6 and S7); extended reaction times did not lead to further uptake. While FTIR and ^{13}C CPMAS NMR spectra (Supporting Information, Figures S1 and S3) of the capped POFs showed definite increases in imine bonds, there were still a significant number of unreacted groups, suggesting that some of these may not be accessible to the capping agent. Analysis of the end-capped POFs suggested an upper limit of approximately 20−30% of each type of functional groups that remained unreacted in the as-synthesized POF samples (Supporting Information, Tables S3−S7).

Thermogravimetric analysis of a dried sample of POF **A1-B2** shows that it is stable up to ~400 °C, a characteristic shared by all the POFs listed in Table 1 (Supporting Information, Figure S37). SEM analysis of all these POFs reveal a general morphology that is best described as aggregates of nanoparticles (Supporting Information, Figures S38 and S39). X-ray diffraction profiles of these microporous polymers do not contain any sharp signals, indicating that they are amorphous random networks, with absence of long-range order.

The N_2 adsorption−desorption isotherms (Figure 3a) of POFs **A1-B2** (Table 1, entries 2a and 2d) suggest that they are mainly microporous, given the high uptake of nitrogen at low pressure. The presence of larger pores (i.e., >20 nm) is also indicated by the steep upward-sloping trend of the isotherm at higher pressures (P/P_0 > 0.9), which reveals the presence of interparticle porosity. The minimal hysteresis in these profiles suggests that adsorption and desorption are equally facile. Pore size distribution analysis for POF **A1-B2** (Table 1, entries 2d), performed using non-local density functional theory (NLDFT), confirm a primary pore width of 6 Å (Figure 3b). Interestingly, even though the synthesized POFs are amorphous, their pore size distributions are not wide (Supporting Information, Figures S33−S36).

Given their ability to retain small gas molecules, lightweight, and very high surface area, microporous organic polymers have been explored as possible future materials for hydrogen storage.[8,23−27] For this application, POFs

(23) Budd, P. M.; Butler, A.; Selbie, J.; Mahmood, K.; McKeown, N. B.; Ghanem, B.; Msayib, K.; Book, D.; Walton, A. *Phys. Chem. Chem. Phys.* **2007**, *9*, 1802–1808.
(24) Germain, J.; Hradil, J.; Fréchet, J. M. J.; Svec, F. *Chem. Mater.* **2006**, *18*, 4430–4435.
(25) Lee, J. Y.; Wood, C. D.; Bradshaw, D.; Rosseinsky, M. J.; Cooper, A. I. *Chem. Commun.* **2006**, 2670–2672.
(26) Satyapal, S.; Petrovic, J.; Read, C.; Thomas, G.; Ordaz, G. *Catal. Today* **2007**, *120*, 246–256.
(27) Wood, C. D.; Tan, B.; Trewin, A.; Niu, H.; Bradshaw, D.; Rosseinsky, M. J.; Khimyak, Y. Z.; Campbell, N. L.; Kirk, R.; Stöckel, E.; Cooper, A. I. *Chem. Mater.* **2007**, *19*, 2034–2048.

Table 2. Surface Areas and Pore Properties of Imine-Linked POFs Analyzed by CO_2 and N_2 Adsorption[a]

entry	polymer[b]	specific surface area ($m^2\ g^{-1}$)	micropore volume ($cm^3\ g^{-1}$)	total pore volume ($cm^3\ g^{-1}$)	yield (%)
1	**A1-B1**[c,e]	335[h] (N_2: 443)[i]	0.13[h] (N_2: 0.14)[i]	0.32	89
2	**A1-B2**[c,e]	529[h] (N_2: 1063)[i]	0.21[h] (N_2: 0.31)[i]	1.13	98
3	**A1-B4**[d,f]	370[h] (N_2: 129)	0.15[h] (N_2: n.a.)[g]	n.a.[g]	87
4	**A1-B5**[d,f]	296[h] (N_2: 63)[i]	0.12[h] (N_2: n.a.)[g]	n.a.[g]	88
5	**A1-B6**[d,f]	259[h] (N_2: 50)[i]	0.10[h] (N_2: n.a.)[g]	n.a.[g]	85

[a] Values in parentheses are obtained from N_2 adsorption measurements. [b] All reactions were carried out at 0.48 M aldehyde functional group concentration. [c] Reactions were carried out in DMSO. [d] Reactions were carried out in DMF. [e] Both monomers were combined together at the beginning of the reaction, which was then heated at 180 °C for 24 h (Condition I). [f] A solution of the amine monomer was slowly added to a trialdehyde solution over 25 min at 50 °C at the beginning of the reaction, and the resulting mixture was heated at 180 °C for 24 h (Condition III). [g] The solids obtained have negligible N_2-uptake. [h] Data obtained from the CO_2 adsorption measurement at 273 K. [i] Data obtained from the N_2 adsorption measurement at 77 K.

A1-B2 (Table 1, entries 2a and 2d) were found to possess H_2 adsorption capacities in the range of 1.2 and 1.5 wt %, at 1 bar and 77 K (Figure 4a). The H_2 adsorption measurement performed for POF **A1-B2** (Table 1, entry 2d), at high pressures and 77 K, shows an increase in H_2 uptake with the increase in pressure giving maximum H_2 uptake of 4.3 wt % at 70 bar (Figure 4b). These H_2 adsorption capacities are comparable to the observed values for unmodified MOFs,[28] and microporous carbon materials with similar specific surface area.[8,27,29] The heats of H_2 adsorption for these two samples of POFs **A1-B2** were calculated to be 8.0 and 8.2 kJ mol^{-1}, respectively, at low coverage, falling to 3.0 and 2.1 kJ mol^{-1}, respectively, at atmospheric pressure (Supporting Information, Figures S28 and S31).

Combining **A1** with *meta*-diamines **B3**−**B6** allows us to introduce alkyl, hydroxyl, and iodo substituents into imine-linked POFs to study the effects of these functional groups on pore properties. In DMSO and under conditions in which both the monomers are added in the beginning, only the [**A1** + **B3**] combination afforded POF **A1-B3** with relatively high surface area (723 $m^2\ g^{-1}$) (Table 1, entry 3). The other combinations only yielded black non-porous solids, presumably because of oxidation by DMSO. Thus, the reactions of **A1** with **B4**−**B6** were repeated in DMF to afford POFs **A1-B4** through **A1-B6** as brown powders with moderate BET surface areas for N_2 adsorption (Table 2, entries 4−6).

Curiously, POFs **A1-B4** through **A1-B6** exhibit significantly higher surface areas when evaluated by CO_2 adsorption (using Dubinin−Radushkevich model).[30] Their CO_2-accessible surface areas are comparable to that of the non-functionalized POF **A1-B1**, which has 3−8 times higher surface area for N_2 adsorption using the BET method. This suggests that while the functional groups in the former POFs may have reduced the N_2-accessible pores, the presence of functional groups does not affect the total CO_2-acccesible micropore volume.

Conclusion

In conclusion, we have shown that thermally stable imine-linked microporous POFs can be synthesized in a facile manner using readily accessible and abundant monomers. By proper tuning of reaction conditions, monomer structure, and rate of reactant addition, surface areas as high as 1500 $m^2\ g^{-1}$ can be achieved. The promising H_2 and CO_2 adsorption data obtained for these materials suggest that they have good potential as media for gas storage applications. In addition, the presence of functional groups in the pores should allow for selective recognition applications and gas separation.

Acknowledgment. We gratefully acknowledge the U.S. DOE-EERE (Grant DE-FG36-08GO18137/A001) for financial support. Instruments in the Northwestern University Integrated Molecular Structure Education and Research Center (IMSERC) were purchased with grants from NSF-NSEC, NSF-MRSEC, Keck Foundation, the state of Illinois, and Northwestern University. We thank Brad G. Hauser for help with the high-pressure hydrogen adsorption measurements. We acknowledge the use of instruments at the Electron Probe Instrumentation Center (EPIC) and Keck Interdisciplinary Surface Science (Keck-II) Center facilities at Northwestern University.

Supporting Information Available: Synthetic procedures, FTIR data, TGA data, ^{13}C CPMAS NMR data, nitrogen, carbon dioxide, and hydrogen adsorption isotherms, heat of adsorption calculations, pore size distribution graphs, and SEM images. This material is available free of charge via the Internet at http://pubs.acs.org.

(28) Mulfort, K. L.; Hupp, J. T. *J. Am. Chem. Soc.* **2007**, *129*, 9604–9605.
(29) Felderhoff, M.; Weidenthaler, C.; Helmolt, R. v.; Eberle, U. *Phys. Chem. Chem. Phys.* **2007**, *9*, 2643–2653.
(30) Garrido, J.; Linares-Solano, A.; Martín-Martínez, J. M.; Molina-Sabio, M.; Rodriguez-Reinoso, F.; Torregrosa, R. *Langmuir* **1987**, *3*, 76–81.